

## FEDSM-ICNMM2010-30892

### MECHANICAL PROPERTIES OF TUBE-SHAPED POLY (VINYL ALCOHOL) HYDROGEL BLOOD VESSEL BIOMODEL

**Hiroyuki KOSUKEGAWA**

Graduate School of Engineering, Tohoku University  
Sendai, Miyagi, Japan

**Shuya SHIDA**

Graduate School of Biomedical  
Engineering, Tohoku University  
Sendai, Miyagi, Japan

**Yoko HASHIDA**

Institute of Fluid Science,  
Tohoku University  
Sendai, Miyagi, Japan

**Makoto OHTA**

Institute of Fluid Science,  
Tohoku University  
Sendai, Miyagi, Japan

#### ABSTRACT

Biomodels, which mimic the shape and motion of blood vessels, have been developed for clinical training in endovascular intervention and for the technical development of interventional devices such as stents. The present authors have developed a biomodel made of poly (vinyl alcohol) hydrogel (PVA-H), which has good transparency, low surface friction, and dynamic viscoelasticity similar to that of arteries. However, evaluation of its behavior as an arterial biomodel has not been carried out. In order to develop a PVA-H biomodel which can accurately mimic the motion of blood vessels, it is necessary to measure and match its mechanical properties in a tube shape mimicking blood vessels. In this study, tube-shaped PVA-H biomodels were prepared, and their mechanical properties were evaluated as to pulse wave velocity (PWV), compliance, and transfer function.

PWV was calculated with Young's modulus and dimensions of the biomodels. A tube-shaped PVA-H model and a model made of commercial silicone were set in a pulsatile flow path apparatus filled pure water (23°C). Sinusoidal pulsatile waves of various frequencies generated by a screw pump were released into flow path. The flow rate, the inner pressure, and the diameter of the biomodels were measured. The compliance of a biomodel was calculated with changing pressures and diameters. The transfer function was obtained as the ratio of the amplitude of the pressure in front of a biomodel and that behind it.

The two kinds of biomodels studied showed PWV similar to that of real arteries: PVA-H shows lower PWV which younger arteries tend to show, while silicone shows higher PWV, similar to the case of aged arteries. In compliance, PVA-H shows a value similar to that of arteries in the lower pressure range, whereas silicone shows a value similar to that of arteries

at higher pressure. A difference of transfer function in relation to the pulsatile frequencies was observed. This phenomenon is similar to that of real blood vessels and explainable in terms of the theory of the forced vibration in single-degree-of-freedom systems with attenuation. The transfer function is affected by mechanical properties of the wall, and the difference between biomodels is due to the viscoelasticity of the biomodels. With PVA-H, these parameters can be gradually changed by adjusting factors such as concentration. These findings indicate that PVA-H would be useful for the development of biomodels.

#### INTRODUCTION

Blood vessel biomodels, which are functional models mimicking the shape and motion of blood vessels, have been developed for clinical training in endovascular intervention (1, 2). The reason why biomodels are desirable is that advanced skill and considerable experience are required of the interventionalists who maneuver some small devices in the human body. This kind of model is useful not only for the training of intervention but also for preoperative simulation and informed consent. In addition, biomodels with realistic mechanical properties and geometrical structures can also contribute to the mechanical study of blood vessels or blood flow. Furthermore, biomodels can be useful for technical evaluation of interventional devices. In fact, considerable research has been done using biomodels, particularly silicone models, to investigate mechanical action of blood vessels or blood flow (3 – 10).

Recently, a biomodel mainly made of poly (vinyl alcohol) hydrogel (PVA-H) has been developed (2 – 5), (11, 12). PVA-H is a useful material because it has such good transparency that interventionalists can easily see the situation inside the biomodel. In addition, it also has low surface friction (2) like

## Nomenclature

L	Length
W	Width
$D_{out}$	Outer diameter
$D_{in}$	Inner diameter
$D'_{out}$	Initial outer diameter at $P = 0$ mmHg
$D'_{in}$	Initial inner diameter at $P = 0$ mmHg
$\epsilon$	Strain
E	Young's modulus
h	Thickness of the wall
$\rho$	Density of fluid
$P_1$	Pressure in front of the specimen
$P_2$	Pressure behind the specimen
$P_m$	Mean pressure of $P_1$ for over four seconds
Q	Flow rate
C	Compliance
S	Cross-sectional area of biomodel
$A_{P1}$	Amplitude of $P_1$
$A_{P2}$	Amplitude of $P_2$
v	Wave speed
t	Elapsed time
$t_w$	Cycle time of pulsatile flow at 1 Hz

living tissue due to its highly water content. Kosukegawa et al. have reported that the dynamic viscoelasticity of PVA-H is quite similar to that of real human arteries (11). Thus, PVA-H may be suitable as a material for biomodels. However, the mechanical properties and other aspects of PVA-H in applicative shape have not yet been reported. In this study, in order to evaluate the behavior of an applicative PVA-H biomodel, the behavior and mechanical properties of a tube-shaped PVA-H biomodel were evaluated.

In many cases, researchers and medical personnel often take note of some parameters such as pulse wave velocity (PWV) (13, 14) or compliance (15 - 17) to evaluate the stiffness of blood vessels. For example, deterioration of PWV and the compliance due to arteriosclerosis become larger than that of a healthy vessel because the vessel wall has become stiffer. Medical personnel can diagnose whether the examinee is suffering from vascular disease from the vessel parameters. These days, besides PWV and compliance, blood vessels and blood flow can be also evaluated based on its pressure and flow profile. The transfer function in pressure between two different parts of a vessel is a parameter which is well related to wave profiles (18 - 21). It is strongly dependent on frequency, and can possibly be used for clinical diagnosis. Representation of the frequency dependence of mechanical properties of blood vessels is important for the development of a biomodel. It can contribute to the reproduction of phenomenon inside a blood vessel such as the blood flow pattern when clinical devices are used. These facts indicate that realistic PWV, compliance, and transfer function should be incorporated in a biomodel to mimic the behavior and action of actual blood vessels. In this study,

tube-shaped biomodels were measured to evaluate the mechanical properties, i.e., PWV, compliance, and transfer function.

## METHODS

### Materials

Mechanical properties of three kinds of tube-shaped specimens (PVA-H, silicone, acrylic pipe) with similar dimensions were examined. A tube-shaped PVA-H was obtained by using PVA powder with a 1700 degree of polymerization and with a saponification value of 99 mol%. The concentration of PVA-H was 18 wt.%, which shows viscoelasticity similar to that of an animal artery. A commercial silicone tube (Super Tex tube, SK Co., Ltd.), which is used for conventional biomodels, was employed as a lower elastic commercial silicone model. Acrylic pipe, a rigid material, was used as a control.

### Preparation of Tube-shaped Poly (vinyl alcohol) Hydrogel

A tube-shaped PVA-H was prepared by applying the method proposed previously (11, 12). First, the proper amount of PVA powder (JF17, JAPAN VAM & POVAL Co., Ltd.) was added to a dimethyl sulfoxide (DMSO) aqueous solution (80 wt.%), and dissolved at 100°C for 2 hours. The concentration of PVA in the solution was 18 wt.%. After PVA powder had dissolved in the solution, an aluminum cylinder ( $L = 250$  mm,  $D_{out} = 4.0$  mm) was inserted into an acrylic pipe ( $L = 250$  mm,  $D_{in} = 6.0$  mm), and the solution was flowed into the space between the pipe and cylinder. Both ends of the space were then sealed with two short silicone rubber tubes ( $D_{out} = 6.0$  mm,  $D_{in} = 4.0$  mm). The solution inside the pipe was put in a freezer at -30°C for 24 hours to promote gelation. After gelation, a tube-shaped PVA gel including DMSO was obtained by pulling the gelled PVA-H out with the acrylic pipe at room temperature. In order to replace DMSO with water as a solvent, the resulting PVA gel was immersed in ethanol at room temperature for 24 hours and then immersed in pure water for over four days. This swelling procedure requiring immersion for more than 4 days is due to the fact that the swelling value of PVA-H can be equilibrated 4 days after immersion (22).

### Measurement of Dimensions of PVA-H Specimens

Because of the swelling of hydrogel, the dimensions of PVA-H should be measured after the immersion. Image processing by using a camera (FASTCAM SA3, Photron Ltd.) was employed for the measurement of the dimensions of each biomodel. All biomodel specimen cut out from the tube-shaped models were fixed on a flat stage, and several pictures of the cross section of each tube-shaped specimen were captured by camera with a resolution of 15.2  $\mu\text{m}/\text{pixel}$ . The images were processed with a software package (Vision Assistant, National Instruments Co.), and the initial dimensions ( $D'_{out}$  and  $D'_{in}$ ) of each specimen were calculated (Table 1).

### Pulse Wave Velocity

To calculate the PWV of each biomodel, Young's modulus of each model was first measured by a single-axis tensile test using a tensile tester (EZ-S, Shimadzu Co.). Each biomodel was cut into rectangular shape ( $L = 50$  mm,  $W = 10$  mm). The specimens were stretched at a constant rate of 20 mm/min to strain ( $\epsilon$ ) of 1.0 and returned to a strain of 0.0. Repeating these cycles three times, Young's modulus of the biomodel was

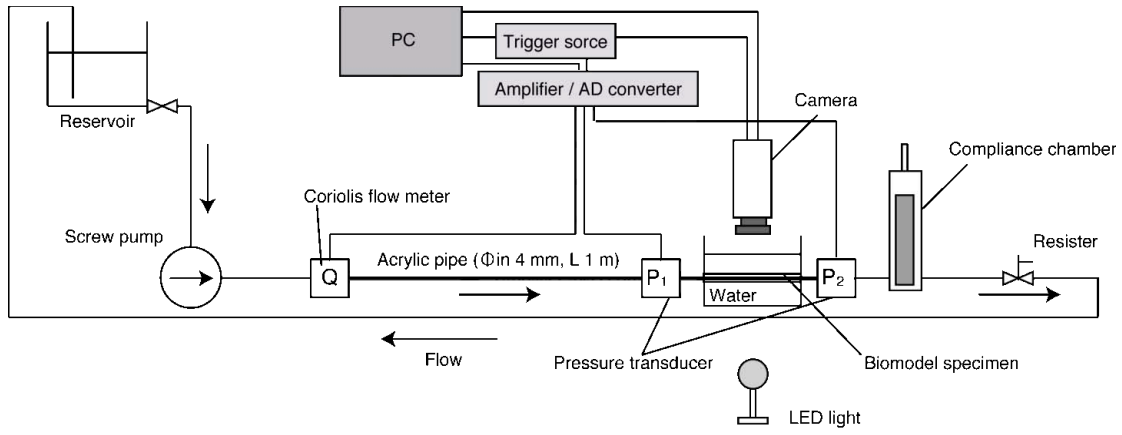


**Figure 1** Schematic drawing of a pulsatile flow apparatus. All parts except for the specimen were made of acrylic. Each pressure transducer was at a distance of 80 mm from the specimen. Data acquisition from pressure transducers, flow meter, and camera was synchronized by a trigger signal. The flow path in the range from the Coriolis flow meter to the resistor was kept flat, and the diameter of the path was 4 mm.

**Table 1** Dimensions of biomodels and acrylic pipe

	$D_{out}$ [mm]	$D_{in}$ [mm]
PVA-H	6.15 ± 0.16	4.23 ± 0.10
Silicone	6.05 ± 0.07	3.84 ± 0.04
Acrylic pipe	6.08	4.00

defined as the value obtained by dividing stress by the strain at  $\epsilon = 0.1$  in the third cycle.

The pulse wave is transmitted on the vessel during expansion of the wall. Therefore, the PWV can be calculated using the elasticity, thickness of wall, and the density of fluid. In general, PWV can be calculated by the following equation (Eq. 1). In this study, the PWV of the biomodel was theoretically obtained by applying proper values of thickness in Eq. 1.

$$v = \left( \frac{Eh}{\rho D_{out}} \right)^{1/2} \quad (1)$$

### Pulse Wave Profile, Compliance, Transfer Function

Many researchers construct a proper flow system to investigate the physics or simulation of blood flow, or for the technical evaluation of endovascular devices with biomodels. In this study, tube-shaped biomodels and an acrylic straight cylinder were cut, and fixed on the flow system shown in Fig. 1. The length of the unattached portion of the biomodels was 98 mm. The model was loaded with sinusoidal pulsatile flow of various frequencies. After working fluid (pure water of 23°C) was flowed into a screw pump (R'Tech Co., Ltd.), pulsatile flow with a mean flow rate of 840 ml/min was generated by controlling the rotation speed of the rotor of the pump. The flow entered the specimen through a Coriolis flow meter (FD-SS2, Keyence Co.), an acrylic straight pipe ( $D_{in} = 4.0$  mm,  $L = 1.0$  m), and an acrylic connector for pressure transducers (PW-100KPA, Tokyo Sokki Kenkyujo. Co., Ltd.). Two pressure transducers were set in front of and behind the biomodel, and the inner pressures upstream ( $P_1$ ) and downstream ( $P_2$ ) of

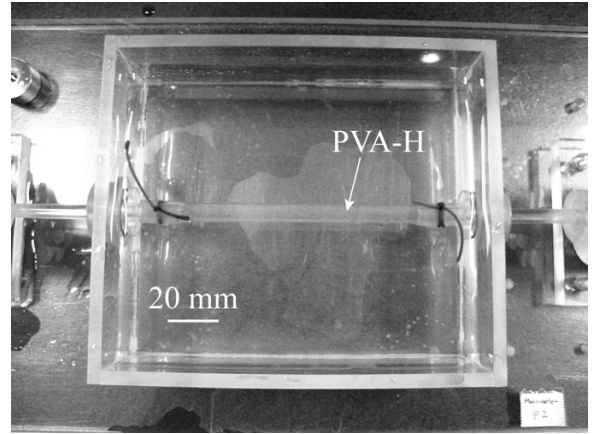


**Figure 2** Tube-shaped PVA-H biomodel fixed in the water tank. Biomodels were tied to the acrylic connectors with rubber strings.

models were measured. After the rear pressure transducer, the flow was returned to the reservoir tank. The mean pressure was controlled with a resistor. Biomodel specimen was fixed in a water tank filled with pure water (Fig. 2).

The change in diameter of the biomodel was measured by image processing. First, the motion of the model was captured with a camera. The captured pictures were processed with a software package (LabVIEW ver.8.5, National Instruments Co.), and the outer diameter ( $D_{out}$ ) was obtained. Then, the inner diameter ( $D_{in}$ ) of the model was calculated by Eq. 2 assuming Poisson's ratio of the biomodel to be 0.5. Flow rates ( $Q$ ),  $P_1$ ,  $P_2$ , and  $D_{in}$  were measured for over four seconds at a time resolution of 1 ms, and ensemble average values for each second were obtained.

$$D_{in} = \sqrt{D_{out}^2 - (D'_{out}{}^2 + D'_{in}{}^2)} \quad (2)$$

From the pressure and diameter profiles at 1 Hz, the diameter-pressure curve of the biomodel was obtained. The

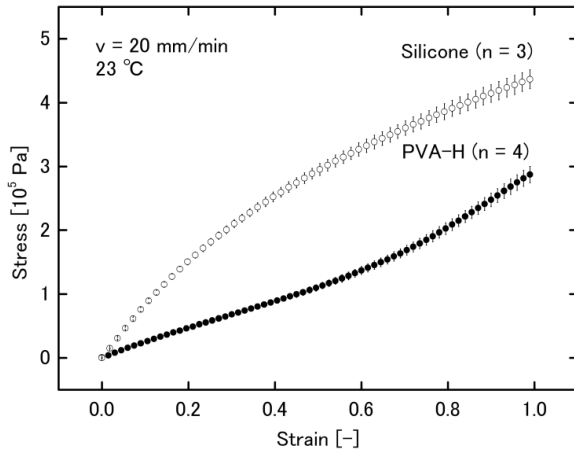


**Figure 3** Stress-strain curve and Young's modulus of biomodels

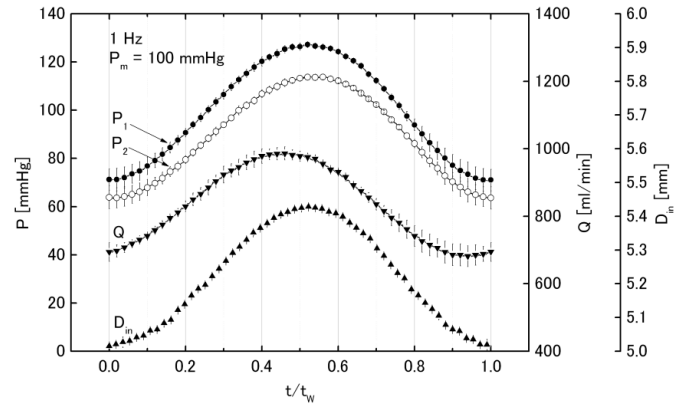


**Figure 4** Pressure, flow rate, and diameter profiles of PVA-H at  $P_m = 100$  mmHg at 1 Hz (Average  $\pm$  SD of 4 samples). Abscissa axis means the normalized time by the cycle time of a 1 Hz.

**Table 2** Young's modulus and PWV of biomodels.  $E_{0.1}$  is Young's modulus at a strain of 0.1. Each value is an average  $\pm$  SD in  $n = 4$

- ※ 1 Measured dimensions of each biomodels are from Table 1
- ※ 2 ( $D_{out} = 6$  mm,  $h = 0.5$  mm. The values are simulated for the dimensions of human artery)

	$E_{0.1}$ [ $10^5$ Pa]	PWV [m/s]	
		Measured dimensions ※1	Simulated dimensions ※2
PVA-H	$2.53 \pm 0.13$	$6.29 \pm 0.16$	$4.59 \pm 0.12$
Silicone	$8.38 \pm 0.28$	$12.39 \pm 0.21$	$8.36 \pm 0.14$

compliances ( $C = d(D_{in}^2) / 4 dP$ ) of biomodels were obtained from the first derivatives of their approximated curves. In this study, the transfer function between two points of the biomodel was defined as the ratio of the amplitude of  $P_2$  ( $A_{P2}$ ) to that of  $P_1$  ( $A_{P1}$ ). The transfer function was obtained in cases at different frequencies and at different pressures.

## RESULTS

### Pulse Wave Velocity

Figure 3 shows the stress-strain curves of the biomodels. The silicone model shows a typical stress-strain curve for elastomer, while a slight ascending non-linearity is observed in PVA-H. The tendency observed in PVA-H is due to the molecular orientation formed by expansion and compression (23). The curve contour of PVA-H, however, did not change even if the expansion-compression cycle was repeated. Young's modulus and the PWV of biomodels are shown in Table 2, and the PWV is calculated for two cases, one with measured dimensions and the other with simulated dimensions ( $D_{out} = 6$  mm,  $h = 0.5$  mm). The silicone employed in this study has higher elasticity than PVA-H even though it is softer than commercial silicone. Because of its higher elasticity, the PWV of silicone is twice as high as that of PVA-H in the same dimension.

### Pulsatile Flow Profiles

In order to evaluate the behavior of biomodels and acrylic pipe, the pressure upstream and downstream of the specimen, and the diameter change were measured. Figure 4 shows the pressure, flow rate, and diameter profiles of PVA-H at 1 Hz. In this pulsatile flow apparatus, the peak flow rate is before that of pressure and diameter. The peak of  $P_2$  is slightly delayed from that of  $P_1$  by about 19 ms. This value can be calculated from PWV and the length of PVA-H. The peak of  $D_{in}$  is almost the same or slightly delayed from that of  $P_1$ .

Figure 5 shows the diameter-pressure curve of biomodels obtained at 1 Hz. The two tube-shaped biomodels show the linear relationship of the curve, and the compliance was obtained from the gradient of their approximate linear fitting curves. PVA-H shows a compliance 10 times that of silicone.

Figure 6 shows the pressure-time profile of PVA-H in  $P_m = 100$  mmHg in pulsatile flow. The amplitude of  $P_1$  ( $A_{P1}$ ) and that of  $P_2$  ( $A_{P2}$ ) decrease with the increase of frequency because quick vibration of the pump rotor can allow a small amount of fluid transfer. In addition, the phase between  $P_1$  and  $P_2$  at 1 to 4 Hz is close, while it seems to be reversed at 8 Hz. This phenomenon is observed in all specimens.

On the other hand, the transfer function is changeable and dependent on the frequency, as shown in Fig. 7. The dependence on frequency is observed in all specimens, especially noticeable in PVA-H. In all cases, the transfer

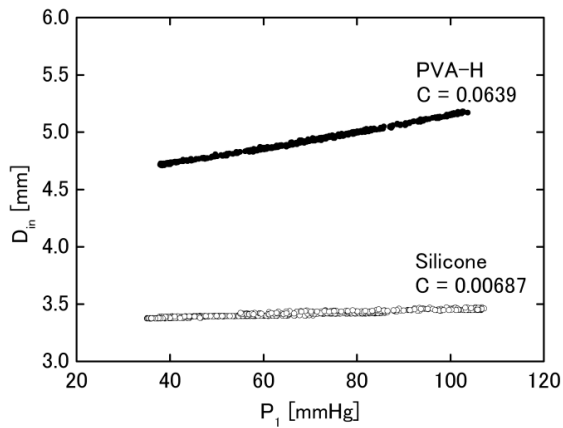


**Figure 5** Diameter-pressure curve of biomodels. Compliance ( $C$ ) is given as in  $\text{mm}^2/\text{mmHg}$

function becomes the highest at 4 Hz and PVA-H is 1.5 to 2 times the ratio compared to silicone and acrylic pipe (Fig.8). Figure 9 shows the transfer function against mean pressure. Silicone and acrylic pipe has almost no dependence on pressure in transfer function, whereas PVA-H shows clear dependence especially at higher frequency.

## DISCUSSION

PWV, compliance, and transfer function of biomodels and rigid material, parameters which have been well examined in previous cardiovascular studies, were investigated, and two kinds of materials, PVA-H and silicone, used for biomodels were evaluated. Many researchers have reported those parameters of human arteries in relation to ages, region, or health condition. According to their reports, the PWV of *in vivo* human arteries generally ranges from about 4 m/s to 12 m/s (13, 24 – 26). Table 2 indicates that the PWV of biomodels used in this study can mimic that of *in vivo* human arteries, even though it is necessary to consider that the wall thickness of a biomodel is different from that of a human artery. Several researchers (24 – 26) have reported that the PWV of human arteries tends to increase with age. The PWV of arteries of young people (e.g., 10 to 29 years old) is about 4 m/s to 7 m/s, whereas that of aged arteries (e.g., over 50 years old) is 7 m/s to 12 m/s as measured between the carotid and femoral arteries. Karamanoglu et al. have reported the difference of PWV according to the location of the blood vessel (20). According to their report, the aorta and proximal artery show low PWV and the distal artery shows high PWV. Even younger arteries, e.g. most distal arteries, have a PWV of more than 9 m/s. Considering these reports, the results of this study indicate that PVA-H tends to have a lower PWV like that of younger or proximal arteries, while silicone has a higher PWV like that of older or distal arteries. The other possible factor affecting PWV is wall thickness, and thus in the development of biomodels, it is important to reproduce the wall thickness of real blood vessels. In order to reproduce the PWV of artery with real wall thickness, it would be necessary to control the elasticity of the model by changing one of its components, for example, concentration or degree of polymerization. The mechanical properties of PVA-H are capable of being controlled gradually and extensively by various methods (11).

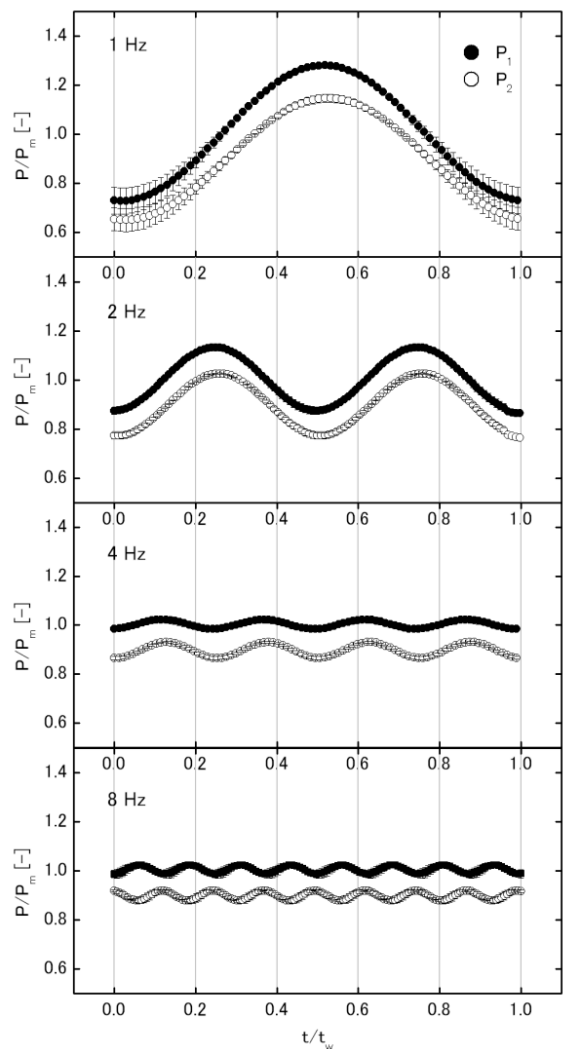


**Figure 6** Pressure profiles of tube-shaped PVA-H at frequencies of 1 - 8 Hz (Average  $\pm$  SD of 3 or 4 samples). Black plots are  $P_1$  and white ones are  $P_2$ . Vertical axis means the pressure ( $P_1$ ,  $P_2$ ) normalized by mean pressure  $P_m$ , and the abscissa axis means the normalized time.  $P_m$  is near 100 mmHg.

Therefore, PVA-H can mimic various PWV, even the higher PWV of older arteries, by adjusting the wall thickness.

Unlike the case of real blood vessels, the compliances of both PVA-H and silicone are almost constant and have a non-linear relationship in the diameter-pressure curve. However, PVA-H can reproduce the compliance of an artery at lower inner pressure (e.g., less than 80 mmHg), and silicone has similar compliance to artery at higher pressure (e.g. more than 120 mmHg). In order to represent the non-linearity of the arterial compliance, the orientation and the hybrid structure would be required for biomodels.

In an experiment on pulse profile, the pressure profile at frequencies from 1 to 8 Hz was observed and evaluated. The reason why this frequency range was employed is because O'Rourke et al. found that most energy of the pressure waves of *in vivo* human arteries is concentrated from 0 to 10 Hz (18).

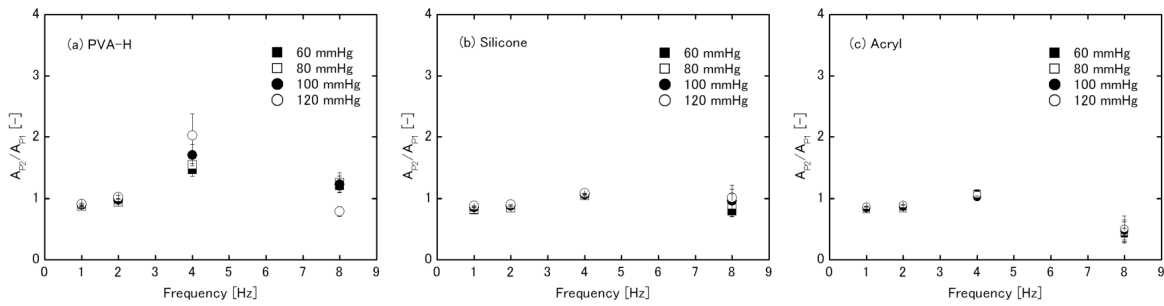


**Figure 7** Transfer function ( $A_{P2}/A_{P1}$ ) against frequency. Abscissa axis means mean pressure of  $P_1$  ( $P_m$ ). (a) PVA-H, (b) silicone, (c) acrylic pipe. (Average  $\pm$  SD of 3 samples)

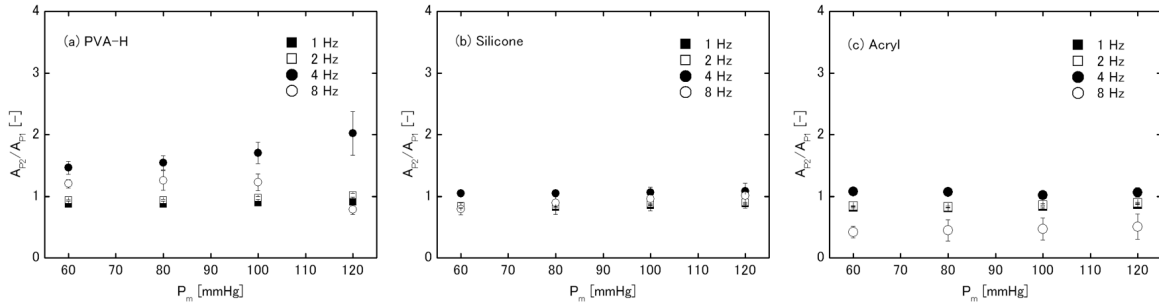


**Figure 9** Transfer function ( $A_{P2}/A_{P1}$ ) against pressure. Abscissa axis means mean pressure of  $P_1$  ( $P_m$ ). (a) PVA-H, (b) Silicone, (c) acrylic pipe (Average  $\pm$  SD of 3 samples)

Karamanoglu et al. reported the transfer function between the ascending aorta and the brachial/radial artery (19 – 21). Their results indicate that an *in vivo* human blood vessel has frequency dependence in the transfer function, the highest value being around 4 Hz. The values found in this study are similar to those of Karamanoglu et al. These results can be explained by considering the forced vibration in single-degree-of-freedom (SDOF) systems with attenuation. From the theory of these systems, the transfer function (magnification factor) becomes largest at the resonance frequency, and decreases at frequencies higher than the resonance point. The curve contour of the amplitude response curve obtained in a blood vessel seems to follow this theory, and the transfer function shows the largest magnification at about 4 Hz due to resonance. Tube-shaped biomodels also show the amplitude response curve. In the theory of forced vibration in SDOF systems, the phase reverses on the boundary of the resonance frequency. In this study as well, the phase tended to reverse between 4 and 8 Hz as shown in Fig. 6. According to this theory and Fig. 6, we can understand that biomodels follow the theory of the forced vibration in SDOF systems with attenuation. Furthermore, the difference of the gain of transfer function is explainable in terms of Young's modulus. According to Karamanoglu et al., an increase of Young's modulus can decrease the gain of transfer function and increase the peak frequency because of viscous attenuation (20). The reason why silicone has a similar gain in transfer function at 4 and 8 Hz in Fig. 8 is because the resonance frequency is higher due to a high Young's modulus. In addition, the viscosity of the wall can also affect the gain of transfer function, and higher viscosity can decrease the gain. Generally, silicone has higher viscosity than PVA-H, which can explain the reason of the results shown in Fig. 8.

Of course, in order to represent the frequency dependence of mechanical properties such as transfer function with biomodels, further investigate of the effect of Young's modulus, viscosity, and reflection from peripheral regions at more detailed frequencies is necessary. These parameters can be easily controlled in PVA-H by adjusting components such as concentrations or saponification values. To represent the frequency dependence of a blood vessel, it is important to simulate the motion of blood vessels and blood flow. Therefore, PVA-H biomodels can possibly contribute to progress in the study of blood flow as well as being a basic training tool for medical devices.

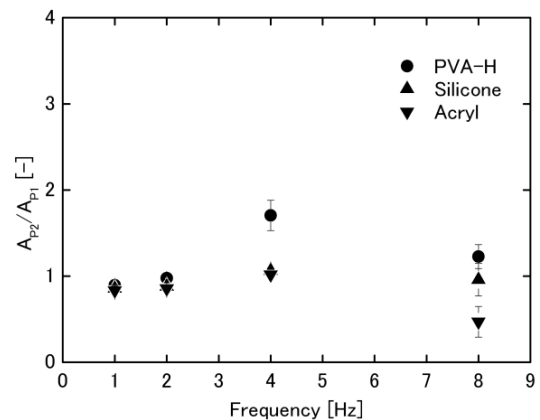


**Figure 8** Comparison of transfer function ( $A_{P2}/A_{P1}$ ) of three kinds of model at  $P_m = 100$  mmHg (Average  $\pm$  SD of 3 or 4 samples)

## CONCLUSION

Biomodels of PVA-H and silicone show different possibilities for mimicking the behavior of blood vessels. PVA-H tends to have a PWV similar to that of proximal or younger arteries, whereas the PWV of silicone is similar to that of distal or older arteries. In compliance, PVA-H has a value similar to that of blood vessels at lower pressure, and silicone has a higher pressure. Besides these frequency-independent parameters, biomodels show the transfer function, which is dependent on frequency. The transfer function of the two biomodels is explainable in terms of the theory of forced vibration in single-degree-of-freedom systems with attenuation. This phenomenon is seen in arteries, and the transfer function is affected by viscoelasticity of the wall. Therefore, in particular, PVA-H can mimic the transfer function of an artery because the viscoelasticity of the model can be controlled.

## ACKNOWLEDGMENTS

This study was supported by a Research Fellowship of the Japan Society for the Promotion of Science for Young Scientists, and by the International Advanced Research and Education Organization of Tohoku University

## REFERENCES

- Ikeda, S., et al., *An in vitro patient-tailored model of human cerebral artery for simulating endovascular intervention*, in *Medical Image Computing and Computer-Assisted Intervention - MICCAI 2005, Pt 1*, J.S. Duncan and G. Gerig, Editors. 2005. p. 925-932.
- Ohta, M., et al., *Poly-vinyl alcohol hydrogel vascular models for in vitro aneurysm simulations: the key to low friction surfaces*. *Technology and Health Care*, 2004. **12**: p. 225-233
- Brusseau, E., et al., *Axial strain imaging of intravascular data: Results on polyvinyl alcohol cryogel phantoms and carotid artery*. *Ultrasound in Medicine and Biology*, 2001. **27**(12): p. 1631-1642
- Fromageau, J., et al., *Characterization of PVA cryogel for intravascular ultrasound elasticity imaging*. *IEEE Transactions on Ultrasonics Ferroelectrics and Frequency Control*, 2003. **50**(10): p. 1318-1324
- Wetzel, S.G., et al., *From patient to model: Stereolithographic modeling of the cerebral vasculature based on rotational angiography*. *American Journal of Neuroradiology*, 2005. **26**(6): p. 1425-1427
- Kitawaki, T., et al., *Effect of the Blood Vessel Viscoelasticity on Periodic Blood Pressure Wave Propagation*. *Journal of Fluid Science and Technology*, 2009. **4**(1): p. 234-245
- Yamaguchi, R., et al., *Velocity profile and wall shear stress of saccular aneurysms at the anterior communicating artery*. *Heart and Vessels*, 2008. **23**(1): p. 60-66
- Yamaguchi, R., et al., *Sinusoidal Variation Of Wall Shear-Stress In Daughter Tube Through 45 Deg Branch Model In Laminar-Flow*. *Journal of Biomechanical Engineering-Transactions of the ASME*, 1994. **116**(1): p. 119-126
- Yamaguchi, R., et al., *Variation of wall shear stress and periodic oscillations induced in the right-angle branch during laminar steady flow*. *Journal of Fluids Engineering-Transactions of the ASME*, 2005. **127**(5): p. 1013-1020
- Tang, D.L., et al., *Steady flow and wall compression in stenotic arteries: A three-dimensional thick-wall model with fluid-wall interactions*. *Journal of Biomechanical Engineering-Transactions of the ASME*, 2001. **123**(6): p. 548-557
- Kosukegawa, H., et al., *Measurements of Dynamic Viscoelasticity of Poly (vinyl alcohol) Hydrogel for the Development of Blood Vessel Biomodeling*. *Journal of Fluid Science and Technology*, 2008. **3**(4): p. 533-543
- Lei Liu, et al., *Anisotropic in vitro vessel model using poly (vinyl alcohol) hydro gel and mesh material*. *Journal of Applied Polymer Science*, 2010. **116**(4): p. 2242-2250
- Learoyd, B.M., et al., *Alterations With Age In Viscoelastic Properties Of Human Arterial Walls*. *Circulation Research*, 1966. **18**(3): p. 278-&
- McEniery, C.M., et al., *Normal vascular aging: Differential effects on wave reflection and aortic pulse wave velocity - The Anglo-Cardiff Collaborative Trial (ACCT)*. *Journal of the American College of Cardiology*, 2005. **46**(9): p. 1753-1760
- Stewart, S.F.C., et al., *Predicting The Compliance Of Small Diameter Vascular Grafts From Uniaxial Tensile Tests*. *Journal of Biomechanics*, 1990. **23**(7): p. 629-637
- Stewart, S.F.C., et al., *Effects Of A Vascular Graft Natural Artery Compliance Mismatch On Pulsatile Flow*. *Journal of Biomechanics*, 1992. **25**(3): p. 297-310
- Tardy, Y., et al., *Noninvasive Estimate Of The Mechanical-Properties Of Peripheral Arteries From Ultrasonic And Phtoplethysmographic Measurements*. *Clinical Physics and Physiological Measurement*, 1991. **12**(1): p. 39-54
- O'Rourke, M.F., et al., *Calibrated ascending aortic pressure waves can be derived from the radial pulse using a generalised transfer function*. *American Journal of Hypertension*, 1999. **12**(4): p. 166A-166A
- Karamanoglu, M., et al., *An Analysis Of The Relationship Between Central Aortic And Peripheral Upper Limb Pressure Waves In Man*. *European Heart Journal*, 1993. **14** (2): p. 160-167
- Karamanoglu, M., et al., *Pressure Wave-Propagation In A Multibranched Model Of The Human Upper-Limb*. *American Journal of Physiology-Heart and Circulatory Physiology*, 1995. **269**(4): p. H1363-H1369
- Nichols, W.W., et al., *McDonald's Blood Flow in Arteries*. 5th ed. 2005, London: Hodder Arnold. 463-502
- Hyon, S., *PVA Hydrogel with intermolecular force*. *Kobunshi Kako*, 1990. **39**: p. 44-50
- Takigawa, T., et al., *Structure And Mechanical-Properties Of Poly (Vinyl Alcohol) Gels Swollen By Various Solvents*. *Polymer*, 1992. **33**(11): p. 2334-2339
- Karnbaum, S., *Elastizitat Und Morphologie Des Aortenwindkessels Beim Bluthochdruck*. *Archiv Fur Kreislaufforschung*, 1961. **34**(1-3): p. 18-&
- Schimmler, W., *Untersuchungen Zu Elastizitatsproblemen Der Aorta (Statistische Korrelation Der Pulswellengeschwindigkeit Zu Alter Geschlecht Und Blutdruck)*. *Archiv Fur Kreislaufforschung*, 1965. **47**(3-4): p. 189-&
- Inagaki, Y., et al., *Arterial Sclerosis and Pulse Wave (in Japanese)*. *Ketsueki to Myakkan*, 1972. **3**(9): p. 43-50